Temperature and doping dependence of the $Bi_{2.1}Sr_{1.9}CaCu_2O_{8+\delta}$ pseudogap and superconducting gap

Azusa Matsuda, Satoshi Sugita, and Takao Watanabe
NTT Basic Research Laboratories, 3-1 Morinosato Wakamiya, Atsugi-shi, Kanagawa 243-01, Japan
(Received 19 June 1998; revised manuscript received 26 March 1999)

The temperature and doping dependence of $Bi_{2.1}Sr_{1.9}CaCu_2O_{8+\delta}$ vacuum tunneling spectra was measured. The tunneling spectra show a clear gaplike feature for almost all the measured temperatures (10–300 K) and doping levels [overdoped ($T_c \sim 80$ K) to underdoped ($T_c \sim 80$ K), via optimum-doped ($T_c \sim 90$ K)]. The superconducting gap structure below T_c develops into a pseudogap above T_c. The model analysis based on the BCS-type density of states showed a sudden increase in the gap value and inelastic scattering rate at T_c. [S0163-1829(99)14825-2]

I. INTRODUCTION

It is well established that the electronic properties of high-T_c cuprates are very different from those of conventional metals. In this respect, the pseudogap phenomenon is one of the most striking features ever observed.[1–3] Recently angle-resolved photoemission spectroscopy (ARPES) experiments[4] have provided direct evidence of the pseudogap opening in the normal state. However, knowledge of the detailed behavior of the pseudogap over the complete temperature-doping level phase diagram is required in order to characterize the pseudogap itself. In the ARPES experiments, unoccupied states cannot be accessed, and hence some characteristic behavior may have been overlooked. Electron tunneling, on the other hand, can provide a single-electron density of state, similar to ARPES, and can also easily probe unoccupied states. Recently, Renner *et al.*[5] reported scanning tunnel microscope (STM) observation of pseudogap formation.

This paper examines the characteristics of the pseudogap by looking at the temperature and doping dependence of the electronic density of states (DOS) in the $Bi_2Sr_2CaCu_2O_8$ (BSCCO) system. BSCCO is a suitable material for tunneling, particularly for a STM study, for the technical reason that a clean surface can be easily obtained. However, it is somewhat difficult to control the doping level without degrading the sample transport properties. We recently succeeded in controlling the oxygen content of BSCCO crystals and hence the doping level without degrading the sample quality.[6] We used an improved annealing process in which an equilibrium oxygen pressure is maintained over almost the whole temperature range during annealing. BSCCO single crystals were grown using a traveling solvent floating zone method. Their actual composition is $Bi_{2.1}Sr_{1.9}CaCu_2O_x$. In the present study, we prepared samples with five different doping levels. All samples were taken from a single boule, which was also used in the transport measurements.[6] The lower curve in Fig. 1 represents T_c as a function of the oxygen content. T_c was determined by resistive and magnetic measurements. In our definition, an oxygen content (x) of 8.25 ($T_c \sim 90$ K) corresponds to optimum doping. T_c varied by at most 10 K for both over- and underdoped sides. Although the T_c variation was relatively small, the corresponding change in the tunneling DOS was significant.

II. EXPERIMENT

We developed a STM unit that can operate at low temperatures in a high vacuum. To approach a sample, we designed an inertial piezoelectric slide with shear piezoelectric devices, which works at low temperature (down to 10 K). Since the sample approach must be repeated almost every time the sample temperature is changed, preciseness is essential for obtaining reproducible data. The STM unit is placed in a vacuum chamber, which is set in a vessel of liquid He. The sample temperature can be changed from room temperature to about 10 K by controlling a heater attached to the sample block, which is loosely heat contacted to a coolant in the vessel.

The sample was cleaved in a flowing N_2 gas atmosphere (not a completely closed condition) and immediately (within several minutes) transferred to the vacuum chamber. The sample was mounted so that the STM tip faced the BSCCO ab plane. The pressure of the vacuum chamber was in the mid-10^{-7}-torr range at room temperature and reached 1×10^{-8} torr when the chamber was cooled. We used mechanically cut Pt-Ir tips and electrochemically etched W tips. Both provide an essentially identical tunneling spectrum. Al-

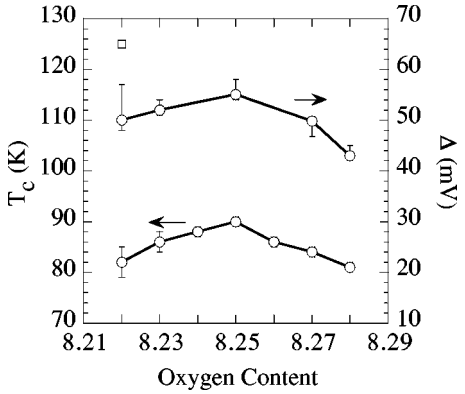

FIG. 1. Oxygen content dependence of T_c and the superconducting gap value ($\Delta = V_{peak}$). The open circles represents the superconducting gap value measured by the tunnel experiment at the lowest temperature. The open square at $x = 8.22$ indicates the gap value at 50 K. The lower curve shows the resistively and magnetically determined T_c.

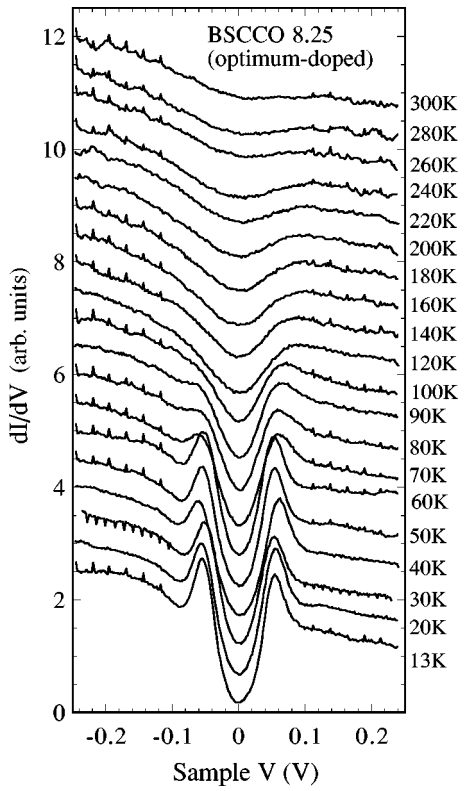

FIG. 2. Temperature dependence of tunneling DOS for the optimum doped sample ($x=8.25$). The tendency of gap formation can be seen even at 300 K. Data are normalized to 2.5 at -250 mV. At the T_c, of the sample, some characteristic changes take place.

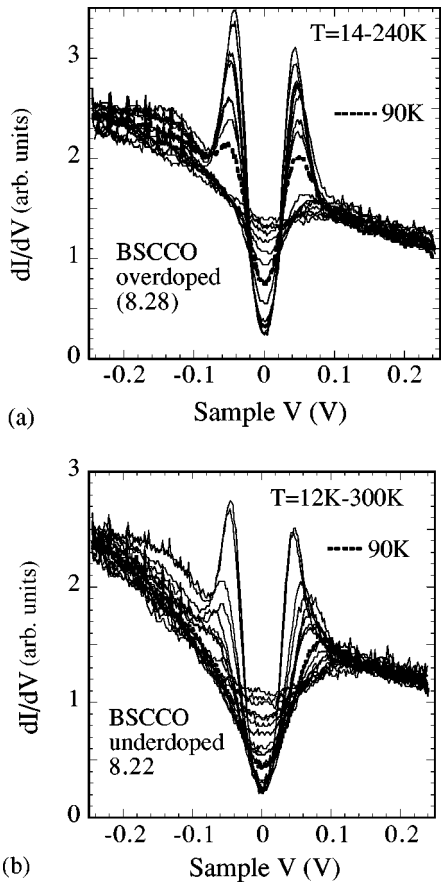

FIG. 3. Temperature dependence of tunneling DOS for (a) the overdoped ($x=8.28$, 14 K$<T<$240 K) and (b) the underdoped sample ($x=8.22$, 12 K$<T<$300 K). All the data were plotted on the same axes.

though our STM has sufficient atomic resolution, which can easily be checked by taking a graphite atomic image, we could not obtain a stable atomic image of the BSCCO surface in the normal tip condition. By using a different UHV STM, in which *in situ* cleaving is possible, we confirmed that cleaving in a flowing N_2 gas causes a problem. However, as far as the tunneling spectrum is concerned, we confirmed that cleaving in a flowing N_2 gas does not cause any essential difference at room temperature. We have also checked that our spectra do not depend on the sample-tip distance

I-V characteristics were acquired by ramping the bias voltage while the feedback loop was cut. To obtain I-V for one place, eight to ten I-V measurements were averaged. The data from five to eight places were averaged again and were numerically differentiated with a finite window. We confirmed that numerical processing does not affect the essential shape of the dI/dV curves, if the sweep voltage is less than ± 250 mV. The I-V were typically taken at $I=0.3$ nA and $V=0.5$ V hence the actual conductance was around several $(G\Omega)^{-1}$. The obtained temperature dependence of the dI/dV curves is plotted as a function of the sample voltage for the optimum-doped sample in Fig. 2 and for the overdoped ($x=8.28$) and underdoped ($x=8.22$) samples in Figs. 3(a) and 3(b). In Fig. 3, all data were plotted without shifting the dI/dV axis. Here dI/dV is proportional to the single-electron DOS. The series of data was normalized so that the positive sides of background DOS coincide with each other. As can be seen, the negative-side background DOS has a rather large temperature dependence. Almost all samples showed an asymmetric background (Fig. 2). However, the sharpness of the gap structure depends in a somewhat uncontrollable way for the underdoped sample on the position of a tip and the measurement conditions. Although we cannot rule out spatial inhomogeneity, we consider that the main cause of such a broadening comes from an additional inelastic tunneling process due to the contamination of the tip. We selected the condition in which the DOS peaks are as sharp as those for optimum and overdoped samples. During the temperature change, we could not trace the same position because of the coarse approach required and because of a large image shift due to thermal expansion.

III. DATA ANALYSIS

A. General characteristics

One of the characteristic features observed in our tunneling spectrum is the apparent asymmetry in the background conductance. In our setup, negative (positive) bias reflects the DOS below (above) the Fermi energy (E_F). This will be discussed in detail elsewhere. Here, we only point out that, according to our doping dependence results, this asymmetry may come from a band structure effect. In the lowest-temperature range (11–14 K) in our STM, the gap structure also depends on the doping. Here, we only present the doping dependence of the gap value Δ, which is half of the distance of the two peaks in energy. This is shown by the upper curve in Fig. 1. The error bars represent the uncer-

tainty possibly due to the spatial inhomogeneity. The gap values are fairly large compared to the BCS value ($2\Delta/kT_c \geqslant 12$).[7] The gap value follows its T_c in the lowest-temperature range. However, the unexpected temperature dependence of the gap in the underdoped sample [see Fig. 5(a)] and possible spatial dependence may invalidate a simple comparison at lowest temperatures. If we take the averaged gap value below T_c or the gap value at higher temperatures (open squares in Fig. 1), it monotonically increases with the decreasing doping level, as reported in other experiments.[5,8,10]

Figures 2 and 3 show that the gap like feature remains above T_c for all doping levels. We identify it as a pseudogap. We define the pseudogap opening temperature T^* at which the normalized DOS (see the following discussion for the definition), at $V=0$, becomes 0.9 times its full value. For samples with $x=8.28$, 8.27 (not shown), and 8.25, T^* is around 220, 270, and 300 K, respectively. In the case of BSCCO, the pseudogap always opens above T_c irrespective of the doping level. This observation is consistent with the STM result of Renner *et al.*[5] but conflicts with several other experiments.[4,9,10] Here we point out two facts which support our observation. We have shown that the BSCCO *c*-axis conduction is governed by a simple tunneling process.[11] Then the *c*-axis resistivity ρ_c should reflect the in-plane DOS. If we define T_0, at which ρ_c starts to increase, then they become 200, 240, and over 300 K.[6] The static spin susceptibility χ_s has a similar tendency. In the case of BSCCO, it starts to reduce at T_m even in the overdoped sample as if the spin excitation acquires a gap.[8] The χ_s measurement of our single crystals shows a T_m of 210, 240, and, 300 K for $x=8.28$, 8.27 and 8.25. The coincidence of T^*, T_0, and T_m is easily understood if one considers that the DOS starts to reduce at T^* as observed in our tunneling measurement. However, break-junction-type tunneling measurements[9,10] show a different behavior, exhibiting no strong evidence of a pseudogap above T_c. The origin of this discrepancy is unknown at the present time and requires further study. The ARPES observations[4] showed that the pseudogap opens only below optimum doping. One of the factors that might prevent ARPES measurements from detecting the pseudogap in overdoped crystals may be the significant asymmetry of the pseudogap structure in energy as seen in Fig. 3(a). The figure shows that only the positive-side DOS, which ARPES cannot probe, retains a detectable BCS-like feature above T_c. This asymmetry develops significantly above T_c.

Besides the above-mentioned asymmetry, two other characteristic changes can be observed at T_c. The BCS-like DOS peak rapidly loses its sharpness and the residual DOS at 0 V rapidly increases at around T_c. These changes can be understood as a rapid increase in the electron inelastic scattering rate due to the disappearance of superconductivity. The pseudogap does not completely suppress the inelastic scattering. The structure appearing at around -150 mV gradually diminishes and finally vanishes at around T_c. The existence of this structure and its disappearance at T_c have been mentioned by many authors.[7,12] Here, we point out that the temperature development is rather gradual and the change may be interpreted in terms of the increase in the scattering rate with increasing temperature. Especially in the underdoped sample [Fig. 3(b)], the peak is rather spread even at the lowest temperature and seems to gradually merge into the background, giving a rather large redistribution of the DOS for the negative side. We cannot distinguish if the structure is accompanied by superconductivity.

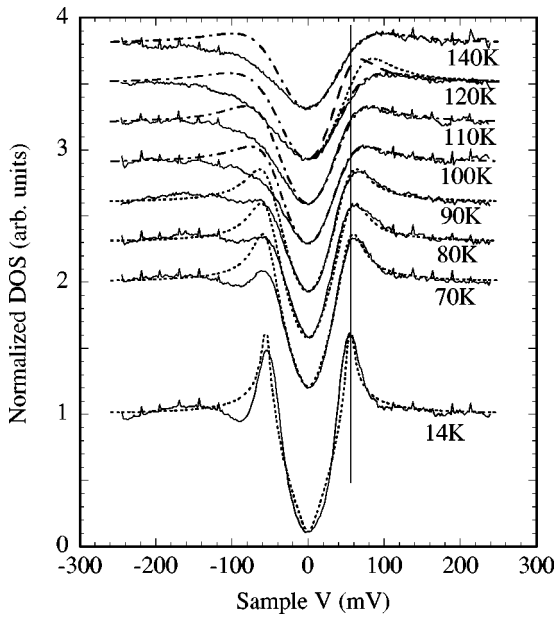

FIG. 4. Temperature dependence of normalized DOS for the optimum-doped sample. The dotted and dot-dashed lines represent results of the BCS fitting with energy-independent and -dependent Γ. The dashed line at 120 K shows the BCS fitting with $\Delta=55$ mV.

B. Analysis using a BCS-type density of states

The systematic temperature evolution of the DOS enables us to analyze the data in a more quantitative way. To do so, we need to subtract the background DOS. Since there is a pseudogap above T_c and there may also be a gradual redistribution of the DOS over a wide energy range, i.e., $\pm$ 500 mV or so, we cannot find an unambiguous way of subtracting the background, which would be available if the gap were absent. Here, we simply construct the background as two linear lines whose slopes are matched to the experimental DOS at around $\pm$ 250 mV. Then we compare the normalized data, which are calculated by dividing the original data by the background, with the smeared BCS-type DOS (Dynes formula). We assume the BCS-type DOS with a *d*-wave symmetry gap for both the superconducting and pseudogap states:[13] $n_0(E)=(1/2\pi)\int d\theta\,\mathrm{Re}[(E-i\Gamma)/\sqrt{(E-i\Gamma)^2-\Delta^2(\theta)}]$, and $n(0)=\int dE n_0(E)[-\partial f(E_f)/\partial E]$. Here, $\Delta(\theta)[=\Delta_{max}\cos(2\theta)]$ is a gap function, Γ is a generally energy- and temperature-dependent scattering rate, and f is a Fermi function. In Fig. 4, the normalized DOS for the optimum-doped sample are plotted together with the results of the BCS fitting. Generally, the fitting becomes worse for lower temperatures and higher doping levels. However, above 70 K, the fittings for the positive side of the DOS become excellent in any case. Above T_c, to account for the sudden decrease in the DOS peak intensity, we consider the additional energy dependence in Γ like $\Gamma(E,T)=\gamma_0(T)+\gamma_1(T)/\{1+\exp[-(|E|-E_0)/W)]\}$, which introduces a step-like increase in Γ at $E=E_0\sim\Delta$. This kind of behavior is expected as a natural consequence of losing true supercon-

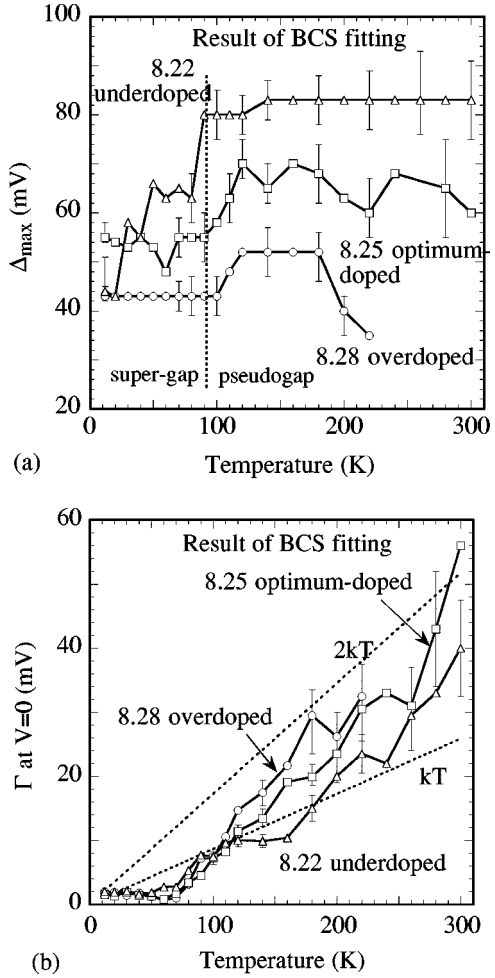

FIG. 5. (a) The fitted results of Δ for several doping levels. (b) The fitted result of Γ at $E=0$. Error bars indicate both spatial variation and fitting uncertainty.

ducting order above T_c. In Fig. 4, the dotted and dash-dotted lines represent the results with an energy-independent and -dependent ($E_0=50$ mV, $W=5$ mV) Γ. At 120 K, both lines are plotted for comparison. Note that our assumed Γ is still suppressed from that expected by the $\Gamma \sim E$ relation at around the gap edge, indicating that not all scattering channels are available at this energy. The introduction of an energy-dependent Γ has very little effect on determining the value of Δ_{max} and Γ at $E=0$. Note that the negative-side DOS deviates systematically from the BCS curves. This does not indicate a poor BCS fitting but suggests the existence of an additional structure in the background DOS. The details of this will be published elsewhere.

In Fig. 5(a), $\Delta_{max}(T)$ obtained as a result of the fitting is plotted for several doping levels. The error bars include both the spatial variation and a fitting uncertainty. In the pseudogap state, the gap value is essentially temperature independent and a monotonically decreasing function of the doping level. We identify it as a pseudogap value. The decrease in the gap of the overdoped sample above 200 K indicates that the gap is closing at this temperature. The Δ_{max} suddenly decreases when the sample goes into the superconducting state for all doping levels. The steplike decrease can be seen in Fig. 4 as an anomalous DOS peak shift at about 100 K. For the 120 K data, the BCS calculation assuming a

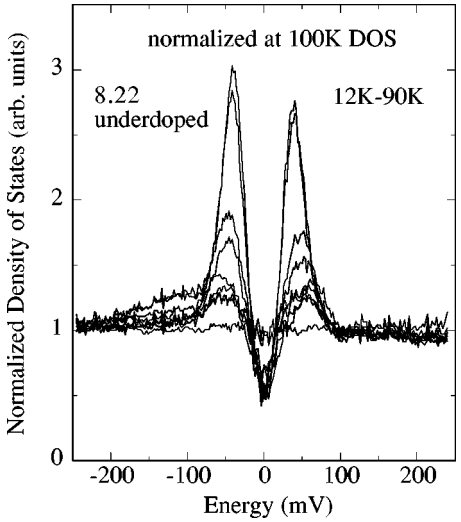

FIG. 6. Temperature dependence of normalized DOS of the underdoped sample below 100 K. In this figure, each DOS was normalized by the DOS at 100 K.

gap the same as that at 14 K (55 mV) is plotted as a dashed line. The apparent difference in the peak position confirms that the steplike increase is a general feature of the data and is beyond the specific analysis used here. The decrease in Δ_{max} below T_c for the underdoped sample looks strange. However, since the DOS at around 2Δ increases with decreasing temperature below T_c, as shown in Fig. 3(b), the superconducting condensation energy may not decrease even in the underdoped sample. This suggests that the gap value is not a good measure of T_c particularly in the underdoped region. Our results here on the temperature dependence of the gap again conflict with superconducting-insulating-superconducting (SIS) tunneling measurements,[9,10] while vacuum tunneling measurements[5] support our results. The origin of this difference in behavior between STM and SIS break junctions requires further investigation. One may consider that the pseudogap is a sort of a band structure either of the Bi-O or the Cu-O electronic system and that the strongly energy-dependent background alters the DOS peak position. However, it is very unlikely because if we normalize the DOS in the superconducting state by that of just above T_c, as shown in Fig. 6, the shape of the superconducting gap structure becomes far from acceptable. The resulting DOS gives a very small dip for $|V|<\Delta$, while gigantic peaks at $|V|=\Delta$. Our data suggest that the pseudogap is continuously replaced by the superconducting gap at T_c. The interpretation of the pseudogap as a superconducting fluctuation seems to be inadequate since the pseudogap is apparently larger than the superconducting gap. Note that the pseudogap value becomes comparable to the spin exchange energy J.

In Fig. 5(b), $\Gamma(0,T)$ is plotted for several doping levels. In our samples, Γ was suppressed to a small value compared to kT, below T_c. However, when superconductivity is lost, it begins to increase as expected. The Γ in the pseudogap state shows a T linear dependence and falls between the $2kT$ and kT line. It is consistent with the inelastic scattering rate derived from the transport measurements.

IV. SUMMARY

In summary, the tunneling spectra show a clear gaplike feature for almost all measured temperatures (10–300 K) and

doping levels [overdoped ($T_c \sim 80$ K) to underdoped ($T_c \sim 80$ K), via optimum-doped ($T_c \sim 90$K)]. The gap structure below T_c develops into a pseudogap above T_c with some characteristic changes at T_c. The pseudogap opening temperature T^* coincides with the temperature at which *c*-axis resistivity shows a characteristic upturn and static susceptibility starts to decrease. An analysis based on BCS-like DOS showed that the pseudogap is larger than the superconducting gap. The temperature dependence of the gap value exhibits very different behavior when compared to that of the BCS relation.

ACKNOWLEDGMENTS

We would like to thank Takenori Fujii for his sample characterization and Dr. Kouichi Semba and Dr. Michio Naito for their valuable discussions.

[1] H. Yasuoka, T. Imai, and T. Shimizu in *Strong Correlation and Superconductivity*, edited by H. Fukuyama, S. Maekawa, and A. P. Malozemoff (Springer, Berlin, 1989), Vol. 89, p. 254; W. W. Warren, R. E. Walstedt, G. F. Brennert, R. J. Cava, R. Tycko, R. F. Bell, and G. Dabbagh, Phys. Rev. Lett. **62**, 1193 (1989).

[2] J. Rossat-Mignot, L. P. Regnault, C. Vettier, P. Bourges, P. Burlet, J. Bossy, J. Y. Henry, and G. Lapertot, Physica B **180-181**, 383 (1992).

[3] J. W. Loram, K.A. Mirza, J.R. Cooper, and W. Y. Liang, Phys. Rev. Lett. **71**, 1740 (1993); T. Ito, K. Takenaka, and S. Uchida, *ibid.* **70**, 3995 (1993); D. N. Basov, R. Liang, B. Dabrowski, D. A. Bonn, W. N. Hardy, and T. Timusk, *ibid.* **77**, 4090 (1996).

[4] H. Ding, T. Yokoya, J. C. Campuzano, T. Takahashi, M. Randeria, M. R. Norman, T. Mochiku, K. Kadowaki, and J. Giapintzakis, Nature (London) **382**, 51 (1996); D. S. Marshall, D. S. Dessau, A.G. Loeser, C-H. Park, A. Y. Matsuura, J. N. Eckstein, I. Bozovic, P. Fournier, A. Kapitulnik, W. E. Spicer, and Z.-X. Shen, Phys. Rev. Lett. **76**, 4841 (1996).

[5] C. Renner, B. Revaz, J.Y. Genoud, K. Kadowaki, and Ø. Fischer, Phys. Rev. Lett. **80**, 149 (1998).

[6] T. Watanabe, T. Fujii, and A. Matsuda, Phys. Rev. Lett. **79**, 2113 (1997).

[7] C. Renner and Ø. Fischer, Phys. Rev. B **51**, 9208 (1995).

[8] M. Oda, R. Kubota, K. Hoya, C. Manabe, N. Momono, T. Nakano, and M. Ido, Physica C **281**, 135 (1997).

[9] D. Mandrus, J. Hartge, C. Kendziora, L. Mihaly, and L. Forro, Europhys. Lett. **22**, 199 (1993).

[10] N. Miyakawa, P. Guptasarma, J. F. Zasadzinski, D. G. Hinks, and K. E. Gray, Phys. Rev. Lett. **80**, 157 (1998).

[11] T. Watanabe and A. Matsuda, Phys. Rev. B **54**, R6881 (1996).

[12] M. R. Norman, H. Ding, J. C. Campuzano, T. Takeuchi, M. Randeria, T. Yokoya, T. Takahashi, T. Mochiku, and K. Kadowaki, Phys. Rev. Lett. **79**, 3506 (1997).

[13] G. V. M. Williams, J. L. Tallon, E. M. Haines, R. Michalak, and R. Dupree, Phys. Rev. Lett. **78**, 721 (1997).